

Design of Multi-Band Filters Using Parallel Connected Topology

Sovuthy CHEAB, Peng Wen WONG, Socheatra SOEUNG

Dept. of Electrical and Electronic Engineering, University of Technology PETRONAS, 326100, Tronoh, Perak, Malaysia

sovuthy.cheab@utp.edu.my, wong_pengwen@utp.edu.my, socheatra@gmail.com

Submitted May 25, 2017 / Accepted November 5, 2017

Abstract. *This paper presents the design of multi-band filters using parallel connected topology. The resonator in each branch is the dual-mode resonator which provides two resonant modes per passband for miniaturization. The coupling values of the resonator are obtained by mapping the filtering function of the dual-mode resonator to the second order Chebyshev polynomial. The control of the filter parameters, such as pass-band bandwidths and band separation, is addressed. Dual-band and triple-band filter prototypes are designed and fabricated to validate the proposed concept. The measured results show good agreement with the simulations.*

Keywords

Dual-band, dual-mode, multi-band filter, parallel connected topology, stepped-impedance resonator (SIR), transmission zero (TZ), triple-band

1. Introduction

With the ever-increasing demand for application flexibility, more wireless systems are leaning towards dual-band and multi-band operation, multi-band filter, mostly dual-band filter, becomes one of the hottest topics in microwave filter design nowadays. The multi-band filters appear thereby as one of the solutions to optimize the size and cost of such multi-functional systems. One of the application examples is the high speed wireless local area networks (WLANs) standards such as IEEE 802.11b/g (2.4/2.45 GHz) and IEEE 802.11a (5.2–5.8 GHz) specifications have been developed. One method to form a dual-band bandpass filter is to insert a bandstop filtering response in between a wide passband to divide it in two passbands [1]. This introduces the transmission zeros within the passband to achieve the desired bands. The main disadvantage of this method is that it still needs tuning and optimization process after the combination of the bandpass and bandstop. Moreover, the two passbands could not be far apart from each other. Other techniques of dual-band filter designs had also been introduced in [2]. However,

these techniques do not possess the control of rejection level between the dual-bands and are substantially based on the numerical optimization. An analytical approach based on simultaneous bandpass and bandstop frequency transformation was introduced but the method involves indirect synthesis technique for the construction of a filter limited to dual-band bandpass response [3], [4]. A dual mode microstrip fractal resonator is proposed in [4] and optimized perimeter of the proposed resonator by using fourth iteration T-square fractal shape. To form a multi-band bandpass filter, several bandpass filters having different resonant frequencies are combined together. In [5], [6], parallel networks (that use single-mode resonators) have been used in switchable multiplexer. The required embedded RF switches in these designs degrade the passband insertion loss. The back-to-back star junction topology has also been reported for the design of a triplexer and multiplexers [7–10].

In this paper, multi-band filters using parallel connected topology will be introduced and discussed. The proposed multi-band configuration has the ability to design each passband separately. Therefore, it is possible to choose any desired center frequency of each passband and not just limited to the application for suppressing interference between two or more closely spaced channels. With the introduction of source-load coupling, additional two transmission zeros (TZs) are obtained on both sides of each passband. The position of TZs in between the two passbands can be brought closer to each passband to provide the higher isolation by just providing an appropriate source-load coupling. It is worth mentioning that the similar design has been also proposed not for a multi-band filter but for a single band dual-mode filter where the theory of parallel connected network is given [11]. The organization of this paper is as follow. Section 2 introduces the proposed multi-band resonator followed by the discussion of its analysis and the dual-mode resonator lowpass prototype where the coupling values are extracted. At the end of this section is the discussion of spurious performance of the dual-mode resonator. Section 3 discusses on the design principle of the multi-band filter. Section 4 demonstrates the designed examples where microstrip and coaxial line prototypes are designed, fabricated, and measured to prove the feasibility of the approach. Section 5 is the conclusion.

2. Proposed Multi-Band Filter

Consider the parallel connected network shown in Fig. 1 where each subnetwork is symmetrical and has different transfer characteristic. The subnetwork can be formed by having one, two, or more dual-mode resonators. N is the number of branches. For this analysis, the subnetwork is formed by incorporating a stepped-impedance dual-mode resonator whose impedance ratio is chosen to be a_i . The coupling between the source/load (input/output) to the resonators are K_i where $i = 1, 2, \dots, N$ whereas K_{SL} is the source-load coupling which is used to achieve, according to minimum path rule [12], [13], the maximum number of TZs. The overall transfer characteristic can be evaluated by adding the Y -parameters respectively as

$$Y_{11} = \sum_{i=1}^N \frac{(1 - S_{11,N}^2) - 2 S_{21,N}}{\Delta S_N} \quad (1)$$

where

$$\Delta S_N = (1 - S_{11,N})^2 - S_{21,N}^2. \quad (2)$$

The new transfer characteristic is given by

$$S_{21} = \frac{2 Y_{21}}{\Delta Y} \quad (3)$$

where

$$\Delta Y = (1 - Y_{11})^2 - Y_{21}^2. \quad (4)$$

Considering the subnetwork $Y_{\text{sub}1}$ with stopband window $\Delta\omega_s$ (refer to Fig. 2), where $S_{11,1} \approx 1$ and $S_{21,1} \approx 0$ and let $N = 2$,

$$S_{21} \approx \frac{2 Y_{21,2}}{\Delta Y_2} = S_{21,2}. \quad (5)$$

Hence it is suggested that the summing operation can be achieved by having the parallel connected network.

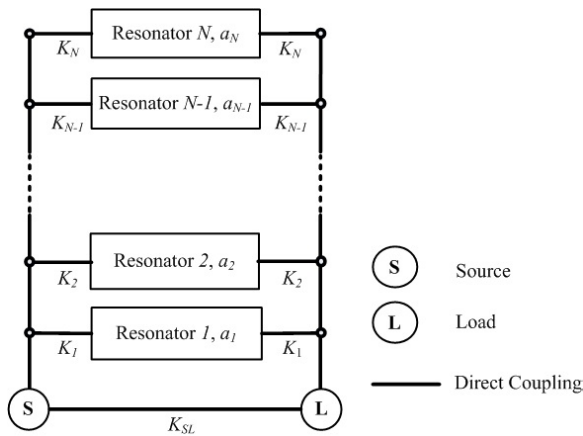


Fig. 1. Proposed multi-band topology.

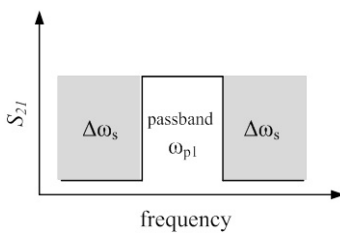


Fig. 2. Transfer function characteristic.

2.1 Dual Mode Resonator

The resonator used in each branch is the stepped-impedance dual-mode resonator [14]. The resonator is comprised of transmission line section loaded with lumped coupling element L shunted at the midpoint as depicted in Fig. 3. The odd- and even-mode equivalent circuits are shown in Fig. 4a and Fig. 4b.

The odd-mode condition is given as

$$Y_{\text{odd}}|_{=0} = 1 - a \tan^2(\theta). \quad (6)$$

Or

$$\theta = \arctan \sqrt{\frac{1}{a}}. \quad (7)$$

The odd-mode resonant condition suggests that the odd-mode resonance can be controlled by the impedance ratio a and it is not affected by the inductor. Modeling an inductive element by a shorted circuit stub with characteristic impedance aZ and a very short electrical length $\Delta\theta$, the input admittance for even-mode at resonance is given by

$$Y_{\text{even}}|_{=0} = 1 - a \tan(\theta) \tan(\theta + \Delta\theta). \quad (8)$$

For a very small real number α , $\Delta\theta$ can be expressed as

$$\Delta\theta = \alpha \theta. \quad (9)$$

Hence (8) becomes

$$Y_{\text{even}}|_{=0} = 1 - a \tan(\theta) \tan[\theta(1 + \alpha)]. \quad (10)$$

It can be shown that with a finite value of α or an appropriate inductor, an even mode resonance takes place close to the odd mode resonance. Therefore, the resonator gives dual-mode response. This means that the inductor can be used to couple between the even- and odd-mode resonances.

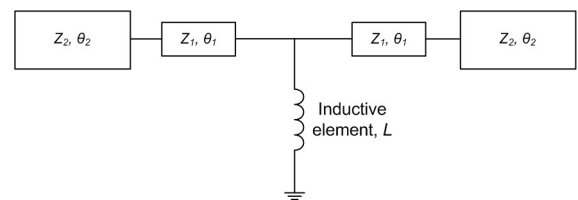


Fig. 3. Stepped-impedance dual-mode resonator.

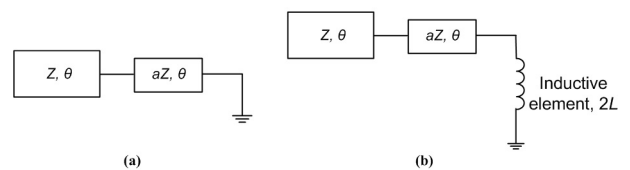


Fig. 4. Odd- and even-mode equivalent circuits.

2.2 Spurious Frequency Performance

Suppose the fundamental passband resonance and lowest spurious resonance frequency are expressed in terms of f_0 and f_s , respectively, the following relationship is obtained

$$f_n = \frac{f_0}{f_s} = \frac{\pi}{\arctan\left(\frac{1}{\sqrt{a}}\right)} - 1. \quad (11)$$

Figure 5 plots the normalized spurious resonance frequency. It shows that for uniform impedance resonator (UIR) ($a = 1$) which gives the resonator length of half-wavelength, the spurious frequency appears to be 3 times the fundamental frequency. As the impedance ratio increases, better spurious-free stopband performance is achieved. As an example if $a = 3$, the first spurious resonance frequency appears at five times the fundamental frequency. However, one should consider the practical constraints of impedance value for microstrip which is typically within the range of 20Ω to 200Ω . Note that this remarkable spurious-free stopband performance gives room for many passbands with the following consideration. If UIR ($a = 1$) is used, the maximum frequency separation for the last passband is 3 times of that of the first passband. Consequently, the rest of the passbands should be designed within this range i.e. between the first and the last resonator passbands. Therefore, for wider separated range between passbands or more passbands, the impedance ratio of the first passband resonator to be at least 3 so that the next spurious frequency is at least 5 times its fundamental frequency.

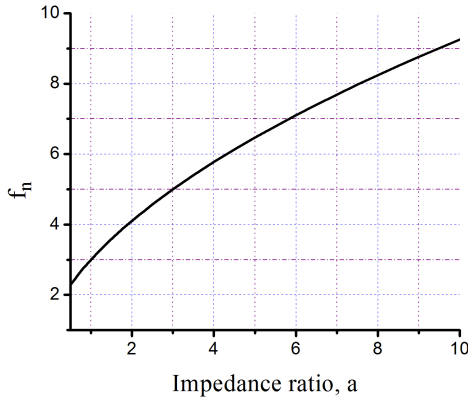


Fig. 5. Normalized spurious resonance frequency.

2.3 Dual-mode Resonator Lowpass Prototype

The routing and coupling structure of the i -th band lowpass dual-mode resonator is depicted in Fig. 6. It comprises of two resonators with an inverter K_{ii} in between. The two resonators are coupled to the source/load by an inverter K_i .



Fig. 6. Coupling and routing structure.

The circuit model is shown in Fig. 7. Assuming the capacitor $C_{i1} = C_{i2} = 1$ F, the cascading elements in Fig. 7 builds up the transfer matrix as

$$[T] = \begin{bmatrix} \omega K_{ii} & j \left(\omega^2 K_i^2 K_{ii} - \frac{K_i^2}{K_{ii}} \right) \\ -j \frac{K_{ii}}{K_i^2} & \omega K_{ii} \end{bmatrix}. \quad (12)$$

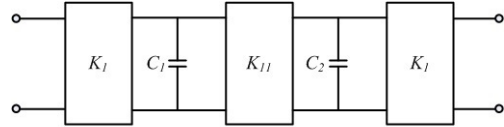


Fig. 7. Lowpass circuit model.

The transfer matrix has been converted to obtain the transfer function whose filtering function can be expressed in terms of K_i , K_{ii} , and ω . This derived filtering function is then mapped to the second order Chebyshev polynomial with 20 dB equiripple in the passband. The mapping gives $K_i = 0.6016602238$ and $K_{ii} = 0.8153692807$. The frequency transformation techniques in [15] can then be applied to the lowpass prototype network to achieve the bandpass at the desired center frequency and bandwidth.

3. Design Principle

Consider Fig. 8 which illustrates the proposed dual-band topology formed by the i -th and j -th resonators. Note that the source-load coupling is not considered. The impedance ratios of the resonator i (lower branch) and resonator j (upper branch) are a_i and a_j respectively. The coupling between the input/output to the resonator i and resonator j are K_i and K_j respectively.

According to (6) and (10), the resonant conditions for even- and odd-mode of the resonator for each branch are given by

$$Y_{\text{odd},i,j}|_{\omega=0} = 1 - a_{i,j} \tan^2(\theta), \quad (13)$$

$$Y_{\text{even},i,j}|_{\omega=0} = 1 - a_{i,j} \tan(\theta) \tan[\theta(1 + \alpha_{i,j})]. \quad (14)$$

The separation of the frequencies $\Delta\theta_{ij}$ can be controlled by the impedance ratio a_i or a_j where,

$$\Delta\theta_{ij} = \theta_{\text{odd},i} - \theta_{\text{odd},j} = \arctan\left(\sqrt{\frac{1}{a_i}}\right) - \arctan\left(\sqrt{\frac{1}{a_j}}\right). \quad (15)$$

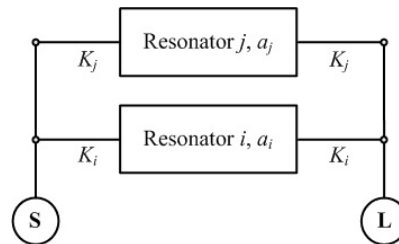


Fig. 8. Dual-band topology formed by the i -th and j -th resonators.

The frequency response in Fig. 9 shows that each resonator is responsible for its filtering passband and hence it can be independently designed to achieve any desired two passbands at different frequencies. The source-load coupling provides a pair of TZs at both sides of each passband resulting in a quasi-elliptic response with enhanced isolation between the two adjacent bands. The coupling underlies the major advantage for high selectivity for this topology since both passband can be further isolated from one another by just controlling the value of the source-load coupling. It should be noticed that an inductive coupling may give TZs too depending on the signs of the K -values and/or coupling between two resonant modes of each resonator.

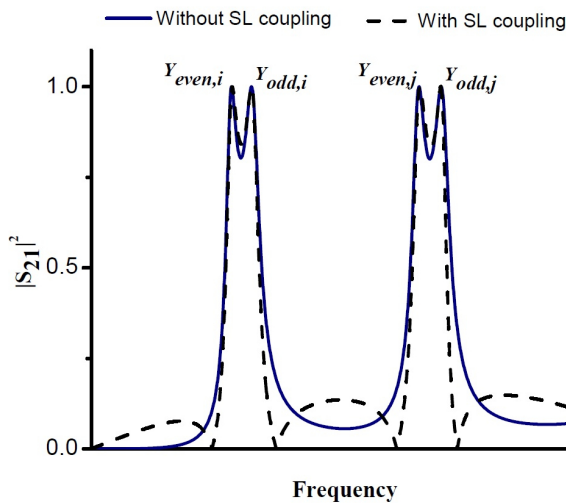


Fig. 9. Frequency response characteristic ($a_i > a_j$).

4. Prototype Design Examples

4.1 Filter I –Dual-Band Filter

The dual band filter microstrip prototype fabricated on Roger RT Duroid 5880 substrate shown in Fig. 10 has been presented in [16] and is shown here to validate the theory. Two pairs of 0.1 pF and 0.2 pF chip capacitors are used to provide the coupling between the input/output to the left hand side resonator and to the right hand side resonator respectively. The source-load coupling is realized by interdigital capacitor. Figure 11 shows the measured and simulated responses of the dual-band dual-mode filter. The first and second passband center frequencies are $f_1 = 2.42$ GHz and $f_2 = 4.99$ GHz respectively. The dual-band filter has four TZs at 2.15 GHz, 2.59 GHz, 4.5 GHz and 5.5 GHz due to the presence of interdigital capacitor. The comparative study of the dual-band filter with other proposed dual-band bandpass filters can be summarized and given in Tab. 1. In this table, h is the substrate height, RL is the passband return loss, IL is the passband insertion loss, ϵ_r is the dielectric constant of the substrate, FBW is the fractional bandwidth and TZ denotes the number of TZs between each passband.

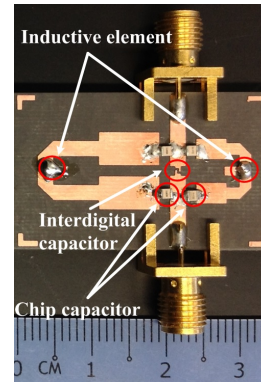


Fig. 10. Microstrip prototype of dual band filter [16].

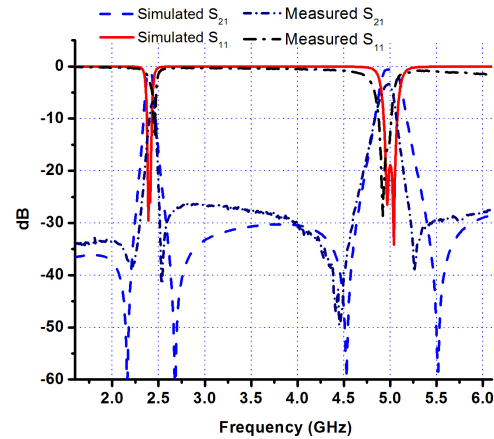


Fig. 11. Measured and simulated responses of dual band filter [16].

4.2 Filter II –Triple-Band Filter

The microstrip prototype for triple band with source-load coupling is designed and fabricated on Roger RT Duroid 5880 substrate with a substrate thickness of $787 \mu\text{m}$, the loss tangent, $\tan \sigma = 0.0009$ and a dielectric constant, $\epsilon_r = 2.2$. The physical layout of the fabricated triple-band filter is shown in Fig. 12. The gaps between resonators to source-load are reserved for the chip capacitors which are required to provide the desired couplings. The total size of the circuit is $1.95 \text{ cm} \times 4.32 \text{ cm}$.

The inductive element is realized by a short circuit via-hole with a diameter of 1 mm shunted at the midpoint of each resonator as shown in Fig. 12. Three pair of chip capacitors used for the source-load and resonator couplings are $c_1 = 0.5 \text{ pF}$, $c_2 = 0.3 \text{ pF}$, and $c_3 = 0.3 \text{ pF}$. The source-load coupling chip capacitor is $c_{\text{SL}} = 0.3 \text{ pF}$. Figure 13 shows simulated and measured S-parameters for the triple band filter. The result shows that the filter gives $\Delta_1 = 66 \text{ MHz}$ at $f_1 = 1.6 \text{ GHz}$, $\Delta_2 = 42 \text{ MHz}$ at $f_2 = 1.9 \text{ GHz}$, and $\Delta_3 = 78 \text{ MHz}$ at $f_3 = 2.3 \text{ GHz}$. The measured insertion loss/return loss are 1.334 dB/13.65 dB at f_1 , 2.466 dB/15.6 dB at f_2 and 1.015 dB/21.35 dB at f_3 respectively. It is noticed that the insertion loss at f_2 is the highest simply due to two factors. First factor is the use of stepped-impedance resonator which results in the reduction of Q and the second factor is the narrowest bandwidth achieved.

Ref.	$h[\mu\text{m}]$	ϵ_r	Passbands*	TZ	RL[dB]	IL[dB]	FBW[%]	Resonator
[17]	580	3.38	2.65/2.44	2	12.6/13	1/2	4.6/4.8	Net-type resonator
[18]	508	3.6	0.9/2.4	0	14/18	2.47/2.8	21/12	Short-circuit terminated SIR
[19]	508	3.38	2.35/3.61	0	17.56/14	0.93/1.13	3.79/2.2	Defected ground structure
[20]	800	2.55	2.4/3.4	0	10/13	2.4/5.2	3/3	Multi-stub loaded resonator
[21]	635	9.5	2.45/5.25	1	13/12	0.9/1.7	4.6/5.1	E-type resonator
[22]	635	6.15	1.84/2.9	2	10/10	1.7/1.6	8.1/6.8	Stub-loaded resonator
Filter B								
[23]	381	2.2	2.45/5.25	2	10/10	2.48/3.55	6/6	Stub-loaded open-loop
Filter II								
Filter I	787	2.2	2.4/5.2	2	12.9/17.3	3.4/6.9	1.25/2	Dual-mode resonator

Tab. 1. Comparisons with other dual-band filters (*frequency in GHz).

Ref.	CFs [GHz]	FBW [%]	TZ*	RL [dB]	IL [dB]	ISO ₁₂ /ISO ₂₃
[24]	1.5/2.45/3.5	7.5/5.8/3.6	0/2	18/17/18	1.17/1.02/2.17	20/20 [dB]
[25]	2.35/4.78/7.86	5.31/6.27/8.66	2/2	12/15/17	1.78/0.9/0.7	14/10 [dB]
[26]	1.5/2.45/3.5	7.3/15.1/8.8	1/1	16/23/23	1.49/0.53/0.7	17/20 [dB]
[27]	1.575/2.4/3.5	5.2/3.8/4.6	1/2	9/18.9/13.5	1.6/1.5/2.3	25/40 [dB]
Filter II	1.6/1.9/2.3	4.13/2.21/3.39	2/2	13.65/15.6/21.35	1.33/2.4/1.02	29/24 [dB]

Tab. 2. Comparison with other reported triple-band filters (*number of TZs between passbands 1-2/2-3).

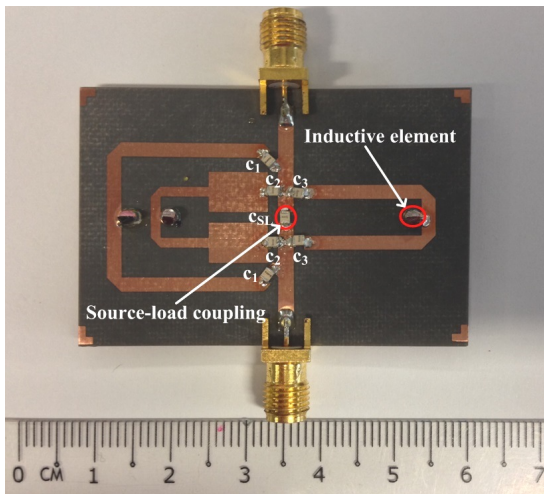


Fig. 12. Microstrip prototype of triple band filter.

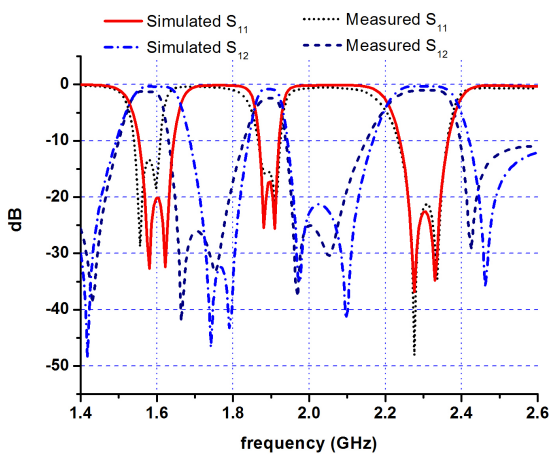


Fig. 13. Measured and simulated responses of triple band filter.

The presence of the chip capacitor for the source-load coupling gives rise to two finite-frequency TZs at both sides of each passband as presented. The six simulated/measured TZs are located at 1.418/1.43 GHz, 1.742/1.664 GHz, 1.79/1.754 GHz, 1.976/1.97 GHz, 2.096/2.054 GHz, and 2.462/2.426 GHz. Hence the filter possesses better advantages of higher selectivity and a good isolation between the the three bands. The location of these TZs can be easily shifted by changing the value of the source-load coupling capacitor. The difference between the measured and simulated result can be attributed to the fabrication tolerance of the vias and the presence of the chip capacitors which result in resonant frequency variation. The isolation between the first and the second passband is 29 dB whereas the isolation between the second and the third passband is 24 dB. The bandwidth of each passband can be made narrower by reducing the value of the inductive element shunted at the midpoint of the respective resonator. Having more via holes i.e. more shunt inductors at the midpoint is one of the effective ways to decrease the value of the inductive element. Table 2 provides a performance comparison with some reported works on triple-band filters. The isolation between the first and the second passband and the second and the third passband are denoted as ISO₁₂ and ISO₂₃ respectively. CF is the abbreviation of center frequency for each passband. It is worth mentioning that extra care in terms of design must be taken for the realizations of filter with more-than-three passbands due to the geometrical limitations of this multi-band filter approach. The inner resonator should be designed for the highest frequency band since it gives the shortest relative length which results in the smallest required footprint. Moreover, the left and right resonators have to be chosen and placed according to the distributed nature of the area where each resonator connects to the input and output ports. Nevertheless, multi-layer design can easily overcome this limitation.

5. Conclusion

In this paper, a novel multi-band filter based on parallel connected topology is proposed and discussed. As an example, a compact dual-mode dual band and triple-band bandpass filters are presented. The dual-band and triple-band filters are made up of two and three parallel connected dual-mode resonators respectively. The source-load coupling provides each filter the advantage of having a quasi-elliptic response. Therefore, the filters are very compact, selective, and with improved isolation. Measured results of the fabricated prototypes show good agreement with simulations and theories.

References

- [1] TSAI, L. C., HSUE, C. W. Dual-band bandpass filters using equal-length coupled-serial-shunted lines and Z-transform technique. *IEEE Microwave Theory and Techniques*, 2004, vol. 52, no. 4, p. 1111–1117. DOI: 10.1109/TMTT.2004.825680
- [2] LEE, J., UHM M. S., YOM, I. B. A dual-passband filter of canonical structure for satellite applications. *IEEE Microwave and Wireless Components Letters*, 2004, vol. 14, no. 6, p. 271–273. DOI: 10.1109/LMWC.2004.828010
- [3] MACCHIRARELLA, G., TAMIAZZO, S. Design techniques for dual-passband filters. *IEEE Microwave Theory and Techniques*, 2005, vol. 53, no. 11, p. 3265–3271. DOI: 10.1109/TMTT.2005.855749
- [4] CAMERON, R. J., YU M., WANG, Y. Direct-coupled microwave filters with single and dual stopbands. *IEEE Microwave Theory and Techniques*, 2005, vol. 53, no. 11, p. 3288–3297. DOI: 10.1109/TMTT.2005.859032
- [5] LAFORGE, P. D., MANSOUR, R. R., YU M. Manifold-coupled switched filter bank implementing filters with embedded switches. In *Proceedings of the IEEE MTT-S International Microwave Symposium Digest*. Atlanta (USA), 2008, p. 1027–1030. DOI: 10.1109/MWSYM.2008.4633010
- [6] MOBBS, C. The use of matched four-port filters to realize switched multiplexer having low amplitude and group delay ripple. *IEEE Microwave Theory and Techniques*, 1987, vol. 35, no. 12, p. 1183–1191. DOI: 10.1109/TMTT.1987.1133836
- [7] TANG, C. W., TSENG, C. T. Design of a packaged microstrip triplexer with star-junction topology. In *Proceedings of the IEEE European Microwave Conference*. Amsterdam (Netherlands), 2012, p. 459–462. DOI: 10.23919/EuMC.2012.6459406
- [8] ZHAO, P., WU, K. L. An iterative and analytical approach to optimal synthesis of a multiplexer with a star-junction. *IEEE Microwave Theory and Techniques*, 2014, vol. 62, no. 12, p. 3362–3369. DOI: 10.1109/TMTT.2014.2364222
- [9] MACCHIRARELLA, G., TAMIAZZO, S. Synthesis of star-junction multiplexers. *IEEE Microwave Theory and Techniques*, 2010, vol. 58, no. 12, p. 3732–3741. DOI: 10.1109/TMTT.2010.2086570
- [10] RHODES, J. D., LEVY, R. A Generalized multiplexer theory. *IEEE Transactions on Microwave Theory and Techniques*, 1976, vol. 27, no. 2, p. 99–111. DOI: 10.1109/TMTT.1979.1129570
- [11] CHEAB S., WONG, P. W., CHEW X. Y. Parallel connected dual-mode filter. *IEEE Microwave and Wireless Components Letters*, 2015, vol. 25, no. 9, p. 582–584. DOI: 10.1109/LMWC.2015.2451393
- [12] CAMERON, R. J. Advanced filter synthesis. *IEEE Microwave Magazine*, 2011, vol. 12, no. 6, p. 42–61. DOI: 10.1109/MMM.2011.942007
- [13] CAMERON, R. J., KUDSIA, C. M., MANSOUR, R., *Microwave Filters for Communication Systems: Fundamentals, Design and Applications*. Hoboken (USA): Wiley-Interscience, 2007. ISBN: 0471450227
- [14] WONG, P. W. Miniaturized stepped-impedance dual-mode resonator filter. In *Proceedings of the IEEE Conference on Microwave Technology & Computational Electromagnetics (ICMTCE)*. Beijing (China), 2011, p. 174–176. DOI: 10.1109/ICMTCE.2011.5915193
- [15] HUNTER, I. *Theory and Design of Microwave Filters*. UK: The Institution of Engineering and Technology, 2001. ISBN: 0852967772
- [16] CHEAB S., WONG, P. W. Compact, quasi-elliptic dual-band bandpass filter with improved isolation. In *Proceedings of the IEEE MTT-S International Microwave Symposium*. Phoenix (USA), 2015, p. 1–3. DOI: 10.1109/MWSYM.2015.7167115
- [17] TSENG, C. H., SHAO, H. Y. A new dual-band microstrip bandpass filter using net-type resonators. *IEEE Microwave and Wireless Components Letters*, 2010, vol. 20, no. 4, p. 196–198. DOI: 10.1109/LMWC.2010.2042549
- [18] CHANG, W. S., CHANG, H. Y. Analytical design of microstrip short-circuit terminated stepped-impedance resonator dual-band filters. *IEEE Microwave Theory and Techniques*, 2011, vol. 59, no. 7, p. 1730–1739. DOI: 10.1109/TMTT.2011.2132140
- [19] KHAJAVI, N., MAKKI, S. V., MAJIDIFAR, S. Design of high performance microstrip dual-band bandpass filter. *Radioengineering*, 2015, vol. 24, no. 1, p. 32–37. DOI: 10.13164/re.2015.0032
- [20] CHEN, F. C., CHU, Q. X. Novel multistub loaded resonator and its application to high-order dual-band filters. *IEEE Microwave Theory and Techniques*, 2010, vol. 58, no. 6, p. 1551–1561. DOI: 10.1109/TMTT.2010.2049161
- [21] ZHOU, M., TANG, X., XIAO, F. Compact dual band filter using novel E-type resonators with controllable bandwidths. *IEEE Microwave and Wireless Components Letters*, 2008, vol. 18, no. 12, p. 779–781. DOI: 10.1109/LMWC.2008.2007696
- [22] ZHANG, X. Y., CHEN, J. X., XUE, Q., et al. Dual-band bandpass filters using stub-loaded resonators. *IEEE Microwave and Wireless Components Letters*, 2007, vol. 17, no. 8, p. 583–585. DOI: 10.1109/LMWC.2007.901768
- [23] MONDAL, P., MONDAL, M. K. Design of dual-band bandpass filter using stub-loaded open-loop resonators. *IEEE Microwave Theory and Techniques*, 2008, vol. 56, no. 1, p. 150–155. DOI: 10.1109/TMTT.2007.912204
- [24] SUN, S. J., SU, T., DENG, K., et al. Shorted-ended stepped-impedance dual-resonance resonator and its application to bandpass filter. *IEEE Microwave Theory and Techniques*, 2013, vol. 61, no. 9, p. 3209–3215. DOI: 10.1109/TMTT.2013.2273895
- [25] LUO, S., ZHU, L., SUN, S. Compact dual-mode triple-band bandpass filters using three pairs of degenerate modes in a ring resonator. *IEEE Microwave Theory and Techniques*, 2011, vol. 59, no. 5, p. 1222–1229. DOI: 10.1109/TMTT.2011.2123106
- [26] WEI, F., QIN, P. Y., GUO, Y. J., et al. Design of multi-band bandpass filters based on stub loaded stepped-impedance resonator with defected microstrip structure. *IET Microwaves, Antennas & Propagation*, 2016, vol. 10, no. 2, p. 230–236. DOI: 10.1049/iet-map.2015.0495
- [27] CHEN, W. Y., WENG, M. H., CHANG, S. J. A new tri-band bandpass filter based on stub-loaded step-impedance resonator. *IEEE Microwave and Wireless Components Letters*, 2012, vol. 22, no. 4, p. 179–181. DOI: 10.1109/LMWC.2012.2187884

About the Authors . . .

Sovuthy CHEAB was born in Battambang, Cambodia, in 1986. He received his BEng (Honors) degree in Electrical and Electronic Engineering majoring in Communication Systems in 2010 from Universiti Teknologi PETRONAS (UTP), Malaysia. He then pursued his MSc and PhD degrees by research in Microwave Engineering and completed both degrees in 2012 and 2015 respectively from the same university. During his PhD studies in UTP, he had also been involved in many communication system design projects including the design of RFID RF front end system. Dr. Cheab has been working as a lecturer in UTP since 2016 in Electrical and Electronic Engineering Department, teaching electromagnetic theory and communication system courses. His research interests include the design and synthesis of microwave filters including multi-mode and multiband filters in both planar and cavity realization. He is currently an IEEE, MTT member, and a committee member of IEEE ED/MTT/SSC Penang Chapter, Malaysia. He also serves as a reviewer for Progress In Electromagnetics Research (PIER) journal.

Peng Wen WONG (M'05 - SM'17) graduated from University of Leeds in 2005 with BEng (1st Class Hons.) degree in Electrical & Electronic Engineering. He received Switched Reluctance Drive Award in EE Engineering. He did his PhD study in University of Leeds, UK from 2007–2009. During his PhD, he was involved in UK DTI funded project, developing process design kits for multilayer system-in-package

modules. Currently he works as Associate Professor in Universiti Teknologi Petronas and received outstanding researcher award in 2013, publication award in 2014 and Potential Academy Award of the Year in 2015. His research interests include reconfigurable filter, lossy filter design, millimeter-wave waveguide filter and passive filter miniaturization techniques. He has secured various research grants from government and industries since 2008 and published more than 60 papers including an article in IEEE microwave magazine. He serves as reviewer for IEEE Transaction on Microwave Theory and Technique, IEEE Wireless & Component Letter, IET Antenna & Propagation and PIERS. He is currently the chair of IEEE ED/MTT/SSC Penang Chapter (2016–2017) and founding chair of IEEE International Microwave, Electron Devices and Solid-State Symposium IMESS 2016. He served as technical chair in IMESS 2017.

Socheatra SOEUNG was born in Phnom Penh, Cambodia, in 1986. He received his BEng (Honors) degree in Electrical and Electronic, major in Computer System Architecture in 2010 from Universiti Teknologi PETRONAS, Malaysia. He completed his MSc degree by research on PCB testing based on Eddy current from Universiti Teknologi PETRONAS, Malaysia in 2013. He is currently pursuing PhD degree by research in RF Microwave Engineering at Universiti Teknologi PETRONAS, Malaysia. His research interests include lossy filter design, passive microwave filter design, and multi-band filter design. He is currently an IEEE, MTT member, and committee member of IEEE ED/MTT/SSC Penang Chapter, Malaysia.